In Vivo Biliary Clearance Should Be Predicted by Intrinsic Biliary Clearance in Sandwich-Cultured Hepatocytes

Masanori Nakakariya, Midori Ono, Nobuyuki Amano, Toshiya Moriwaki, Kazuya Maeda and Yuichi Sugiyama

Drug Metabolism and Pharmacokinetics Research Laboratories, Pharmaceutical Research Division, Takeda Pharmaceutical Company Limited, Osaka, Japan (M.N., M.O., N.A., T.M.)

Laboratory of Molecular Pharmacokinetics, Graduate School of Pharmaceutical Sciences, The University of Tokyo, Tokyo, Japan (K.M.,Y.S.)

1

Running title: Prediction of rat biliary clearance using sandwich culture

Correspondence: Masanori Nakakariya

Drug Metabolism and Pharmacokinetics Research Laboratories, Pharmaceutical Research

Division, Takeda Pharmaceutical Company Limited

26-1, Muraoka-Higashi 2-chome, Fujisawa, Kanagawa 251-8555, Japan

Phone: (+81) 466-32-2869

Fax: (+81) 466-29-4431

E-mail: Nakakariya_Masanori@takeda.co.jp

Number of text pages: 44

Number of tables: 4

Number of figures: 6

Number of references: 35

Number of words in the Abstract: 201

Number of words in the Introduction: 543

Number of words in the Discussion: 1321

Abbreviations: SCRH, sandwich-cultured rat hepatocytes; IVIVC, *in vitro-in vivo* correlation;

BEI, biliary excretion index; Oatp, organic anion transporting polypeptide; Mdr, multidrug

resistance; Mrp, multidrug resistance associated protein; Bcrp, breast cancer resistance protein;

Bsep, bile salt export pump; LC-MS/MS, liquid chromatography tandem mass spectrometry

Abstract

It has been reported that *in vivo* biliary clearance can be predicted using sandwich-cultured rat and human hepatocytes. The predicted apparent biliary clearance ($CL_{bile,app}$) from sandwich-cultured rat hepatocytes (SCRH) based on medium concentrations correlates to *in vivo* $CL_{bile,app}$ based on plasma concentrations of angiotensin II receptor blockers (ARBs), HMG-CoA reductase inhibitors (statins), β-lactam antibiotics, and topotecan. However, the predicted biliary clearance from SCRH was 7- to 300-fold lower than *in vivo* biliary clearance. We speculated that the process of biliary excretion might not have been evaluated using sandwich-cultured hepatocytes. To evaluate this issue, intrinsic biliary clearance ($CL_{bile,int}$) based on intracellular compound concentrations was evaluated to investigate the *in vitro-in vivo* correlation of this process among ARBs, statins, β-lactam antibiotics, and topotecan. Intrinsic biliary clearance in SCRH correlated to *in vivo* values obtained by constant intravenous infusion of 6 compounds, but not rosuvastatin and cefmetazole, to rats. Moreover, differences between SCRH and *in vivo* $CL_{bile,int}$ (0.7- to 6-fold) were much smaller than that of $CL_{bile,app}$ (7- to 300-fold). Therefore, *in vivo* $CL_{bile,int}$ is more accurately reflected using SCRH than $CL_{bile,app}$. In conclusion, to predict *in vivo* biliary clearance more accurately, $CL_{bile,int}$ should be evaluated

instead of $CL_{bile,app}$ between SCRH and *in vivo*.

Introduction

Hepatic clearance is the most important factor governing drug availability because the liver is the primary organ responsible for eliminating xenobiotics in the body. Metabolism, hepatic uptake, and biliary excretion contribute to the elimination of administered drugs. Influx transporters [e.g., organic anion transporting polypeptide (Oatp)] and efflux transporters [e.g., multidrug resistance (Mdr), multidrug resistance associated protein (Mrp), and breast cancer resistance protein (Bcrp)] expressed in the liver play important roles in regulating drug disposition and elimination (Hirano et al., 2004; Hirano et al., 2005; Yamashiro et al., 2006; Nakagomi-Hagihara et al., 2006; Kitamura et al., 2008). Predicting human pharmacokinetics using *in vitro* models and preclinical species efficiently accelerates the process of discovering new drug candidates. Through drug candidate discovery and development, highly accurate forecasting of metabolic clearance has become possible using biological materials (Iwatsubo et al., 1997; Ito et al., 1998). Although biliary excretion is an important route for drug elimination (Levine, 1978; Rollins and Klaassen, 1979), evaluating biliary excretion of drug candidates in humans is difficult due to the scarcity of clinical bile samples. Therefore, it is necessary to predict biliary excretion in humans.

Hepatocytes are a widely accepted *in vitro* tool for evaluating mechanisms of hepatic uptake and metabolism of xenobiotics and hepatotoxicity (Iwatsubo et al., 1997; Kato et al., 2002; Hirano et al., 2005). However, it was reported that cell polarity and liver-specific functions, such as albumin secretion, hepatic uptake, and enzyme activity under conventional monolayer culture conditions were rapidly lost (Foliot et al., 1985; Dunn et al., 1989). In contrast with conventional conditions, sandwich-cultured hepatocytes maintain liver-specific functions for several days and exhibit the formation of bile canaliculi and the localization of efflux transporters on the canalicular membrane (LeCluyse et al., 1994; Talamini et al., 1997). Moreover, the biliary clearance of some drugs, such as angiotensin II receptor blockers, HMG-CoA reductase inhibitors, and β-lactam antibiotics, showed correlation between sandwich-cultured rat or human hepatocytes and *in vivo* (Liu et al., 1999a; Fukuda et al., 2008; Abe et al., 2008; Abe et al., 2009; Li et al., 2010). Although previous reports have suggested that sandwich-cultured hepatocytes can be used to predict the *in vivo* biliary clearance of drug candidates, differences in biliary clearance based on the medium or plasma concentration are greater than 10-fold between sandwich-cultured rat or human hepatocytes and *in vivo* values. This approach may be useful for predicting the rank order of *in vivo* biliary clearance, but

predicting the precision of biliary clearance using sandwich-cultured hepatocytes is questionable.

Since the protein expression of rat Oatp decreases in culture (Hoffmaster et al., 2004; Zhang et al., 2005), decreased influx transporter activities result in differences in biliary clearance between sandwich-cultured rat hepatocytes (SCRH) and *in vivo* for Oatp substrates. In contrast, the protein expression of efflux transporters is relatively maintained during culture (Hoffmaster et al., 2004; Zhang et al., 2005). In several reports, the apparent biliary clearance based on medium concentration was evaluated in SCRH. However, it has not been evaluated whether intrinsic biliary clearance in sandwich-cultured hepatocytes would reflect the process of biliary excretion *in vivo*.

To evaluate this issue, intrinsic biliary clearance based on intracellular concentrations evaluated in SCRH was compared to that based on the concentrations in liver under steady-state conditions by constant intravenous infusion to rats.

Material and Methods

Chemicals

Rosuvastatin and valsartan were purchased from Toronto Research Chemicals, Inc. (North York, Canada). Cefoperazone, diclofenac, and collagenase type I were purchased from Wako Pure Chemical Industries, Ltd. (Osaka, Japan). Cefmetazole and cefpiramide were purchased from the United States Pharmacopeial Convention (Rockville, MD). Pravastatin was purchased from Cayman Chemical Company (Ann Arbor, MI). Topotecan was purchased from Enzo Life Sciences, Inc. (Lausen, Switzerland). Olmesartan was synthesized by Takeda Pharmaceutical Co. Ltd. (Osaka, Japan). Hank's balanced salt solution (HBSS) and Ca^{2+}/Mg^{2+}-free HBSS were purchased from Gibco (Carlsbad, CA). Matrigel and collagen type I-coated 24-well BioCoat plates were obtained from BD Biosciences (Bedford, MA). The hepatocyte plating medium (InVitroGRO CP medium), culture medium (InVitroGRO HI medium), and Torpedo Antibiotic Mix were purchased from Celsis IVT (Baltimore, MD). BCA protein assay kits were purchased from Pierce Protein Research Products (Rockford, IL). All other reagents and solvents were purchased from Wako Pure Chemical Industries, Ltd. (Osaka, Japan) and Sigma-Aldrich Co. (St. Louis, MO).

8

Animals

Male Sprague-Dawley rats were purchased from Charles River Japan Inc. (Shiga, Japan) and acclimatized for more than 7 days before the experiment. Rats were housed in a controlled temperature and humidity with a 12-h light/dark cycle. Laboratory chow (CE-2, CLEA Japan Inc., Tokyo, Japan) and water were available with free access. All animal experiments were conducted in accordance with the guidelines of the Experimental Animal Care and Use Committee of Takeda Pharmaceutical Co., Ltd.

Hepatocyte isolation and culture

Hepatocytes were isolated from male Sprague-Dawley rats by a modification of the two-step collagenase digestion method described previously (Nakakariya et al., 2008). Rats (7-8 weeks) were anesthetized by intraperitoneal injection of pentobarbital. Rat livers were perfused with Ca^{2+}/Mg^{2+}-free HBSS containing 1 mmol/L EGTA for approximate 10 min at a flow rate of 30 mL/min, which was followed by perfusion with HBSS containing 1 mg/mL collagenase type I for approximate 10 min at a flow rate of 15 mL/min. Hepatocytes were

9

dispersed from the digested liver in Krebs-Henseleit buffer with 2% bovine serum albumin and

rinsed by repeated low-speed centrifugation at $50 \times g$ for 5 min at 4°C. The cell pellet was

resuspended in 35% (v/v) isotonic Percoll in Krebs-Henseleit buffer and centrifuged at $100 \times g$

for 20 min at 4°C. After the resultant pellet was resuspended in plating medium, the number

of viable cells was determined using trypan blue staining. Only cells with viability greater

than 90% were used for further studies. Hepatocytes were seeded on 24-well collagen-coated

culture plates at a density of 5×10^5 cells/well in 0.5 mL and allowed to attach for 2 to 3 h at

37°C in a humidified incubator with 95%/5% of air/CO_2. Next, the medium was aspirated, and

the hepatocytes were washed once with plating medium. Fresh plating medium was added to

the cultures. On the second day after hepatocyte plating, hepatocytes were overlaid with BD

Matrigel at a concentration of 0.25 mg/mL in ice-cold culture medium. The culture medium

was refreshed every 24 h for 72 h.

Transport studies in SCRH

The uptake study was carried out using a previously reported method (Liu et al., 1999a).

Briefly, SCRH were rinsed three times with 0.5 mL of HBSS (standard buffer) or

Ca^{2+}/Mg^{2+}-free HBSS with 1 mmol/L EGTA [(–) HBSS], and preincubated in 0.5 mL of

standard buffer or (–) HBSS at 37°C for 10 min.   After removing the buffer by aspiration, an

uptake reaction was initiated by adding 0.5 mL of substrate-containing standard buffer and

terminated by rinsing three times with 0.5 mL of ice-cold standard buffer.   Cells were lysed

with 0.25 mL of 0.5% Triton X-100 in 50 mmol/L phosphate buffer by shaking for

approximately 30 min at room temperature.   Cell lysate samples were mixed with acetonitrile

containing alprenolol and diclofenac at a concentration of 100 ng/mL, which was used as an

internal standard, and then centrifuged.   The supernatants were diluted with an appropriate

volume of 10 mmol/L acetic ammonium or 0.2% (v/v) formic acid in 10 mmol/L ammonium

formate, and analyzed by liquid chromatography with tandem mass spectrometry (LC-MS/MS).

A BCA protein assay kit was used to determine the protein concentration in the cells lysed with

0.5% Triton X-100.

Fluorescence Microscopy.

Retention of 5 (and 6)-carboxy-2′, 7′-dichlorofluorescein (CDF) in bile canalicular lumen was

examined by fluorescence microscopy.   Transport assay was performed using the method

11

described in the section of Transport studies in SCRH. The cells and bile canaliculi were imaged with an inverted fluorescence microscope, CKX41 (Olympus Corporation, Tokyo, Japan).

Determination of plasma protein binding

Plasma protein binding of test compounds was determined using the equilibrium dialysis method. Briefly, 10 µL of 100 µmol/L test compound in DMSO was added to 1 mL of pooled rat plasma to a final concentration of 1 µmol/L. Plasma (150 µL) was placed on one side (plasma side) of a dialysis membrane, and 50 mmol/L phosphate buffer (150 µL) was placed on the opposite side (buffer side). After the tops of both sides were sealed, the plate was placed on a single plate rotator (Harvard Bioscience, Inc., Holliston, MA, 74-2302) set at 20 rpm for 24 h at room temperature, and protected from light. The supernatants were mixed with acetonitrile containing alprenolol and diclofenac at a concentration of 100 ng/mL, which was used as an internal standard, and then centrifuged. Supernatants were diluted with an appropriate volume of 10 mmol/L acetic ammonium or 0.2% (v/v) formic acid in 10 mmol/L ammonium formate, and analyzed using LC-MS/MS.

The unbound fraction in rat plasma ($f_{u,p}$) was calculated using the following equation (eq)

1.

$$f_{u,p} = \frac{C_{buffer}}{C_{plasma}} \qquad (1)$$

where C_{buffer} and C_{plasma} represent the drug concentration on the buffer and plasma sides,

respectively.

In vivo pharmacokinetic studies in rats during continuous intravenous infusion

While under anesthesia induced by isoflurane, 9-week-old rat femoral veins and common

bile ducts were cannulated using 3.0-Fr (ID, 0.61 mm; OD, 0.97 mm) and 2.0-Fr (ID, 0.33 mm;

OD, 0.66 mm) catheters, respectively.   Animals were held in bollman cages during

experiments.   Test compounds were administered at a constant rate (0.2 mL/h) by intravenous

infusion through the femoral vein to achieve a steady-state plasma concentration of compound.

Rosuvastatin, pravastatin, topotecan, cefmetazole, and cefoperazone were dissolved in saline at

a concentration of 1 mg/mL.   Valsartan, olmesartan, and cefpiramide were dissolved in a

mixture of saline and dimethylacetamide (1:1, v/v) at a concentration of 1 mg/mL.   Blood and

bile were collected at designated times, and the blood was centrifuged to obtain plasma.

Livers were collected from sacrificed rats 5 h after beginning the infusion.   Plasma, bile, and

liver samples were frozen at -80°C until analysis.   Plasma, bile and liver samples were mixed

with acetonitrile containing alprenolol and diclofenac at a concentration of 100 ng/mL as an

internal standard, and then centrifuged.   The supernatants were diluted with an appropriate

volume of 10 mmol/L acetic ammonium or 0.2% (v/v) formic acid in 10 mmol/L ammonium

formate, and analyzed using LC-MS/MS.

LC-MS/MS analysis

LC-MS/MS analysis was conducted using an API 4000 triple quadruple mass spectrometer

(Applied Biosystems, Foster City, CA) coupled with a turbo ion spray interface in positive or

negative ion mode and connected to a UFLC (Shimadzu Corporation, Kyoto, Japan).   Reverse

phase chromatography (mobile phase A, 10 mmol/L acetic ammonium for negative ion mode, or

0.2% (v/v) formic acid in 10 mmol/L ammonium formate for positive ion mode; mobile phase B,

methanol) was used to elute and separate the various substrates over a Shim-pack XR-ODS,

C18 column (20 mm × 2.0 mm, 5 μm, Shimadzu Corporation).   Because the chemical structure

of topotecan is pH-dependent, the total amounts of topotecan (lactone and carboxylate form) were determined at an acidic pH. Injections of 10 μL were analyzed at a flow rate of 0.3 mL/min. The following transitions (precursor ion m/z > product ion m/z) were monitored: 480.2 > 243.9 for rosuvastatin, 423.2 > 101.1 for pravastatin, 434.0 > 179.0 for valsartan, 644.1 > 114.9 for cefoperazone, 472.2 > 215.0 for cefmetazole, 613.1 > 122.3 for cefpiramide, 447.3 > 207.2 for olmesartan, 422.0 > 377.0 for topotecan, 250.2 > 116.3 for alprenolol, and 293.8 > 249.9 for diclofenac. Peak areas of all analytes were integrated and quantified using Analyst 1.4.2 (Applied Biosystems).

Data analysis

The biliary excretion index (BEI [%]) and *in vitro* apparent biliary clearance ($CL_{bile,app}$ [mL/h/kg]) were calculated in hepatocytes based on the following equations.

$$BEI = \frac{\text{Accumulation } ((+)Ca^{2+}/Mg^{2+}) - \text{Accumulation } ((-)Ca^{2+}/Mg^{2+})}{\text{Accumulation } ((+)Ca^{2+}/Mg^{2+})} \times 100 \qquad (2)$$

$$\text{In vitro } CL_{bile,app} = \frac{\text{Accumulation } ((+)Ca^{2+}/Mg^{2+}) - \text{Accumulation } ((-)Ca^{2+}/Mg^{2+})}{\text{Incubation time} \times \text{Concentration in medium}} \qquad (3)$$

where accumulation $((+)Ca^{2+}/Mg^{2+})$ and accumulation $((-)Ca^{2+}/Mg^{2+})$ represent the

accumulation of test compounds in SCRH preincubated in standard buffer and (–) HBSS,

respectively. The BEI and $CL_{bile,app}$ were determined after a 15-min incubation. Drug

concentrations in the medium were defined as initial substrate concentration in the incubation

medium. The units of *in vitro* $CL_{bile,app}$ were converted from μL/min/mg protein to mL/h/kg

using the following parameters: rat liver weight and protein content in liver tissue were assumed

to be 40 g/kg body weight and 200 mg protein/g liver weight, respectively (Seglen, 1976;

Davies and Morris, 1993).

The predicted $CL_{bile,app}$ from *in vitro* values were estimated according to the equations

below based on the well-stirred model of hepatic disposition.

$$\text{Predicted } CL_{bile,app} = \frac{Q_p \times \text{in vitro } CL_{bile,app}}{Q_p + \text{in vitro } CL_{bile,app}} \tag{4}$$

where Q_p represents the hepatic plasma flow rate (2268 mL/h/kg).

In eq.4, $f_{u,p}$ was assumed to be unity.

Taking into consideration the unbound fraction,

$$\text{Predicted } CL_{bile,app} = \frac{Q_p \times f_{u,p} \times \text{in vitro } CL_{bile,app}}{Q_p + f_{u,p} \times \text{in vitro } CL_{bile,app}} \tag{5}$$

In vivo $CL_{bile,app}$ were calculated according to eq. 6.

$$\text{In vivo } CL_{bile,app} = \frac{Dose}{AUC_{plasma}} \times \text{\% of dose in bile} \qquad (6)$$

where AUC_{plasma} represents the area under the plasma concentration-time curve. AUC_{plasma}

and % dose in bile values were obtained from references.

The intrinsic biliary clearance ($CL_{bile,int}$), based on the compound concentration in liver and

hepatocytes, was calculated according to eq. 7 (*in vivo*) and 8 (*in vitro*), respectively.

Compound concentration in hepatocytes was calculated based on eq. 9.

$$\text{In vivo } CL_{bile,int} = \frac{X_{bile,\,4h\text{-}5h}}{AUC_{liver,\,4h\text{-}5h}} \qquad (7)$$

$$\text{In vitro } CL_{bile,int} = \frac{\text{Accumulation } ((+)Ca^{2+}/Mg^{2+}) - \text{Accumulation } ((-)Ca^{2+}/Mg^{2+})}{\text{Incubation time} \times \text{Concentration in hepatocytes}} \qquad (8)$$

$$\text{Compound concentration in hepatocytes} = \frac{\text{Accumulation } ((-)Ca^{2+}/Mg^{2+})}{\text{Intracellular space}} \qquad (9)$$

where $X_{bile,4h\text{-}5h}$ and $AUC_{liver,4h\text{-}5h}$ represent the amount of compounds excreted into bile between

4 and 5 h after beginning infusion and the area under the liver concentration-time curve between

4 and 5 h after beginning infusion, respectively. When $CL_{bile,int}$ was compared between SCRH

and *in vivo*, the unbound fraction was presumed to be equal between SCRH and liver.

Therefore, $CL_{bile,int}$ was calculated based on the total concentration of compounds in hepatocytes

and liver.   *In vitro* $CL_{bile,int}$ were determined after 15 min of incubation.   Intracellular space

(5.2 μL/mg protein) was obtained from reference values (Yamano et al., 1999).

Results

Cell morphology and construction of bile canaliculi in SCRH

Figure 1 shows a phase-contrast image of SCRH cultured for 4 days and fluorescence images of SCRH after a incubation with 5 (and 6)-carboxy-2′, 7′-dichlorofluorescein (CDF) diacetate in standard buffer and (–) HBSS. Fluorescent CDF, an Mrp2 substrate, was localized in the bile canalicular lumen after incubation in standard buffer (Fig. 1B). In contrast, CDF was not localized in the bile canalicular lumen, but only intracellular accumulation of CDF was observed in (–) HBSS (Fig. 1C).

Transport study of compounds in SCRH

Eight compounds (rosuvastatin, pravastatin, valsartan, olmesartan, cefmetazole, cefoperazone, cefpiramide, and topotecan) secreted into bile and reportedly observed in *in vitro-in vivo* correlation (IVIVC) were selected to confirm the IVIVC of $CL_{bile,app}$ in SCRH (Fukuda et al., 2008; Abe et al., 2008; Li et al., 2010). Compound accumulations in SCRH are shown in Fig. 2. Accumulation of the test compounds in standard buffer was higher than that in (–) HBSS, except cefmetazole after a 15-min incubation. Table 1 summarizes the BEI and

19

$CL_{bile,app}$ of the test compounds in SCRH. The $CL_{bile,app}$ of the test compounds determined in SCRH was converted to mL/h/kg by determining total protein in each well and using the physiological parameters of the rat (40 g liver/kg body weight and 200 mg protein/g of liver). Nearly all test compound data were similar to reported data (Fukuda et al., 2008; Abe et al., 2008; Li et al., 2010).

IVIVC of apparent biliary clearance in compounds

A well-stirred hepatic model was applied to the predicted $CL_{bile,app}$ from *in vitro* data by eq. 4 and 5, and *in vivo* data were obtained from published data (Tables 1 and 2). When $CL_{bile,app}$ was predicted based on the plasma total concentration of the compound using eq. 4, the predicted $CL_{bile,app}$ did not correlate to $CL_{bile,app}$ *in vivo* (Fig. 3A). However, the predicted $CL_{bile,app}$ based on the plasma unbound concentration of the compound using eq. 5 was correlated to $CL_{bile,app}$ *in vivo* (Fig. 3B), even though the predicted $CL_{bile,app}$ were 7- to 300-fold lower than the *in vivo* $CL_{bile,app}$.

Plasma and liver concentration and cumulative biliary excretion of drugs in rats

To evaluate the $CL_{bile,int}$ based on liver concentration *in vivo*, eight drugs were administered to rats by continuous intravenous infusion. The plasma compound concentration and the biliary excretion-time curves of the test compounds are shown in Fig. 4. Plasma concentration (Fig. 4A) and biliary excretion (Fig. 4B) in 1 h of all the compounds reached steady-state by 4 h after beginning infusion. As shown in Table 3, the $CL_{bile,int}$ *in vivo* calculated using eq. 7 was relatively high for pravastatin and cefoperazone, and low for topotecan.

IVIVC of intrinsic biliary clearance in drugs

The $CL_{bile,int}$ of the test compounds was also evaluated in SCRH using eq. 8, and are summarized in Table 4. The $CL_{bile,int}$ of the test compounds determined in the SCRH was converted to mL/h/kg as well as $CL_{bile,app}$. *In vitro* $CL_{bile,int}$ based on the intracellular total concentration of compound was plotted against *in vivo* $CL_{bile,int}$ (Fig. 5). The $CL_{bile,int}$ in SCRH correlated to that *in vivo* for the 6 compounds tested, except rosuvastatin and cefmetazole. Moreover, compared to the $CL_{bile,app}$ based on the plasma unbound concentration of the compound (7- to 300-fold), differences of $CL_{bile,int}$ between SCRH and *in vivo* were low (0.7- to 6-fold).

Discussion

Biliary excretion is one of the primary elimination routes of xenobiotics and their conjugates, along with metabolism and renal secretion. However, the prediction of biliary excretion in humans using *in vitro* tools has not been established. Recently, it was reported that *in vivo* biliary clearance can be predicted from sandwich-cultured hepatocytes in rats and humans (Liu et al., 1999a; Fukuda et al., 2008; Abe et al., 2008; Abe et al., 2009; Li et al., 2010). Although apparent biliary clearance using sandwich-cultured rat or human hepatocytes correlates to *in vivo* values, the differences in biliary clearance between *in vitro* and *in vivo* are more than 10-fold. Therefore, sandwich-cultured hepatocytes may not be an appropriate method of examining biliary excretion. In the present study, intrinsic biliary clearance based on intracellular concentration was examined in SCRH and *in vivo*, and we found that intrinsic biliary clearance in SCRH could reflect *in vivo* processes.

To evaluate biliary excretion in SCRH, rosuvastatin, pravastatin, valsartan, olmesartan, cefmetazole, cefoperazone, cefpiramide, and topotecan were selected as model compounds. The compounds were excreted into bile canalicular lumen in SCRH, suggesting that functional canalicular transporters expressed and contributed compounds to excrete into bile canaliculi in

22

SCRH (Fig. 2). Next, the IVIVC of apparent biliary clearance based on medium or plasma

concentration of these compounds was evaluated. The correlation between BEI obtained from

SCRH and *in vivo* biliary excretion ratio was not observed (data not shown). Meanwhile, the

predicted $CL_{bile,app}$ with plasma protein binding normalization was correlated with the

corresponding $CL_{bile,app}$ *in vivo* values (Fig. 3B). These results are consistent with published

data (Fukuda et al., 2008; Abe et al., 2008; Li et al., 2010). However, the $CL_{bile,app}$ *in vivo*

values were 7- to 300-fold of the predicted $CL_{bile,app}$ from SCRH (Tables 1 and 2). It was

reported that the hepatic clearance of angiotensin II receptor blockers, HMG-CoA reductase

inhibitors, and β-lactam antibiotics predicted based on uptake clearance in rat isolated

hepatocytes was almost comparable to *in vivo* biliary clearance (Watanabe et al., 2009;

Watanabe et al., 2010a; Watanabe et al., 2010b). These results suggested that the rate-limiting

step of hepatic clearance in these compounds is the hepatic uptake process. In SCRH, protein

expression and uptake activity of Oatp substrates decreased during the culture period (Liu et al.,

1999b; Hoffmaster et al., 2004). In contrast, the protein expression of efflux transporters was

relatively maintained during culture (Hoffmaster et al., 2004; Zhang et al., 2005). Therefore,

differences in apparent biliary clearance between SCRH and *in vivo* may be caused by

decreased influx transporter activity during the culture period.   Thus, the IVIVC of $CL_{bile,app}$ in

test compounds may be reflected in the uptake clearance, and SCRH may not accurately reflect

the biliary excretion process.   To investigate whether $CL_{bile,int}$ is correlated between SCRH and

in vivo, the $CL_{bile,int}$ determined using hepatocytes and liver concentration under steady-state

conditions was evaluated *in vitro* and *in vivo*, respectively.   The intracellular unbound fraction

of test compounds was presumed to be comparable between *in vitro* and *in vivo* when using

similar concentration of compounds; $CL_{bile,int}$ was calculated based on the total concentration of

compounds in liver and hepatocytes (eq. 7 and 8).   The $CL_{bile,int}$ in SCRH correlated to that in

rats for the 6 compounds, except rosuvastatin and cefmetazole (Fig. 5).   Moreover, compared

to $CL_{bile,app}$ based on medium or plasma concentration of the compounds (7- to 300-fold),

differences of $CL_{bile,int}$ between SCRH and *in vivo* were low (0.7- to 6-fold) (Table 4).

There are three possible explanations for the poor correlation of rosuvastatin and

cefmetazole in $CL_{bile,int}$, and the differences of $CL_{bile,int}$ between SCRH and *in vivo*.   First, the

intracellular unbound concentration of compounds in SCRH was different from that *in vivo*.

Second, there was no dynamic blood and bile flow in SCRH.   Finally, efflux transporter

activities changed in SCRH.   For the first possibility, binding components were determined to

be comparable between hepatocytes and liver tissue, and the unbound fraction was presumed to

be equivalent both *in vitro* and *in vivo*.   It was reported that liver to plasma concentration ratio

in vivo was predicted using rat hepatocytes among various compounds *in vitro* (Yamano et al.,

1999).   These results indicated that unbound fraction *in vitro* could be comparable with *in vivo*,

and supported our presumption.   Moreover, there was no possibility of nonlinear unbound

fractions under conditions in which the intracellular compound concentration was nearly equal

in vitro and *in vivo* (Table 4).   These factors rule out the first possibility.   In contrast, the other

two possibilities may have to be taken into account.   The lack of dynamic flow and limited

space of bile canaliculi in the SCRH should result in quick saturation of biliary secretion and

underestimation of biliary clearance.   Figure 6 shows accumulation profiles of rosuvastatin and

pravastatin.   Since the accumulation of these compounds did not change from 3 min after beginning

incubation, time-dependent change of biliary excretion was not observed in SCRH.   However, it

would be difficult to evaluate stably biliary excretion within 3 min for all compounds in practical,

especially valsartan and olmesartan of which BEI is relatively low.   Therefore, a lack of dynamic

flow may cause the differences in $CL_{bile,int}$ between SCRH and *in vivo*.   Transporter expression

levels may also be a determining factor for predicting biliary clearance because transporter

25

mediated hepatobiliary secretion is the predominant route for compound biliary clearance.

Although the decreased protein expression of efflux transporters was lower than that of influx

transporters in SCRH (Hoffmaster et al., 2004; Zhang et al., 2005), the protein expression of

efflux transporters changed by 0.3- to 3-fold during the culture period (Hilgendorf et al., 2007;

Olsavsky et al., 2007).   It was reported that Mrp2 and primarily Bcrp contributes to biliary

secretion of rosuvastatin (Kitamura et al., 2008).   Since Bcrp protein expression increased

during culture, in contrast to the decrease of Mrp2 and Bsep expression (Li et al., 2010),

intrinsic biliary clearance for rosuvastatin is relatively higher than other compounds in SCRH.

Meanwhile, it was reported that Mrp2 mainly contributes to biliary secretion of pravastatin,

ARBs (valsartan and olmesartan) and β-lactam antibiotics (cefoperazone and cefpiramide)

(Kato et al., 2008; Muraoka et al., 1995; Sasaki et al., 2004; Takayanagi et al., 2005; Yamashiro

et al., 2006).   Because the main contributor that excreted rosuvastatin into bile was different

from other compounds, the deviation of rosuvastatin from the correlation among these

compounds would be observed.   Meanwhile, it was reported that cefmetazole was not a

substrate of Mrp2 and Bcrp (Kato et al., 2008).   Although the primary transporter for biliary

excretion of cefmetazole is unknown, it may be possible that the activity change of main

contributors for biliary excretion of cefmetazole caused the deviation of cefmetazole from the

correlation. To overcome these issues, it has been reported that biliary clearance can be

corrected by using the ratio of the protein amount of efflux transporters in rat liver to that in

SCRH, improving the IVIVC of $CL_{bile,app}$ (Li et al., 2010). This correction is more suitably

applied to $CL_{bile,int}$ than $CL_{bile,app}$ because $CL_{bile,int}$ is focused on the process from liver to bile and

involved in efflux transporter activity. In the future, the correction of efflux transporter

activity between SCRH and isolated hepatocytes before seeding should be evaluated. In order

to evaluate the whole hepatobiliary disposition, only SCRH is not appropriate, and elementary steps

of apparent biliary clearance should be evaluated using both SCRH and freshly isolated hepatocytes.

Since it was reported that uptake clearance using freshly isolated hepatocytes would be comparable

hepatic clearance in vivo (Watanebe et al., 2009), the evaluation of uptake clearance using freshly

isolated hepatocytes could be reasonable to cover the defect in SCRH.

In summary, compared to $CL_{bile,app}$ (7- to 300-fold), the absolute values of $CL_{bile,int}$ *in vitro*

were very similar to *in vivo* values (0.7- to 6-fold). This suggests that $CL_{bile,int}$ in

sandwich-cultured hepatocytes can more accurately reflect the process of biliary excretion *in*

vivo than $CL_{bile,app}$. For accurate *in vivo* prediction, $CL_{bile,int}$ should be evaluated instead of

$CL_{bile,app}$ between SCRH and *in vivo*.

Authorship Contributions

Participated in research design: Nakakariya, Ono, Amano, Moriwaki, Maeda, and Sugiyama

Conducted experiments: Nakakariya

Contributed new reagents or analytic tools: not applicable

Performed data analysis: Nakakariya

Wrote or contributed to the writing of the manuscript: Nakakariya, Ono, Amano, Moriwaki,

Maeda, and Sugiyama

30

References

Abe K, Bridges AS, Yue W, and Brouwer KL (2008) In vitro biliary clearance of angiotensin II receptor blockers and 3-hydroxy-3-methylglutaryl-coenzyme A reductase inhibitors in sandwich-cultured rat hepatocytes: comparison with in vivo biliary clearance. *J Pharmacol Exp Ther* **326**:983–990.

Abe K, Bridges AS, and Brouwer KL (2009) Use of sandwich-cultured human hepatocytes to predict biliary clearance of angiotensin II receptor blockers and HMG-CoA reductase inhibitors. *Drug Metab Dispos* **37**:447–452.

Davies B and Morris T (1993) Physiological parameters in laboratory animals and humans. *Pharm Res* **10**:1093–1095.

Dunn JC, Yarmush ML, Koebe HG, and Tompkins RG (1989) Hepatocyte function and extracellular matrix geometry: long-term culture in a sandwich configuration. *FASEB J* **3**:174–177.

Fukuda H, Ohashi R, Tsuda-Tsukimoto M, and Tamai I (2008) Effect of plasma protein binding on in vitro-in vivo correlation of biliary excretion of drugs evaluated by sandwich-cultured rat hepatocytes. *Drug Metab Dispos* **36**:1275–1282.

Foliot A, Glaise D, Erlinger S, and Guguen-Guillouzo C (1985) Long-term maintenance

of taurocholate uptake by adult rat hepatocytes co-cultured with a liver epithelial

cell line. *Hepatology* **5**:215–219.

Hilgendorf C, Ahlin G, Seithel A, Artursson P, Ungell AL, and Karlsson J (2007)

Expression of thirty-six drug transporter genes in human intestine, liver, kidney,

and organotypic cell lines. *Drug Metab Dispos* **35**:1333–1340.

Hirano M, Maeda K, Shitara Y, and Sugiyama Y (2004) Contribution of OATP2 (OATP1B1)

and OATP8 (OATP1B3) to the hepatic uptake of pitavastatin in humans. *J Pharmacol

Exp Ther* **311**:139–146.

Hirano M, Maeda K, Hayashi H, Kusuhara H, and Sugiyama Y (2005) Bile salt export pump

(BSEP/ABCB11) can transport a nonbile acid substrate, pravastatin. *J Pharmacol Exp

Ther* **314**:876–882.

Hoffmaster KA, Turncliff RZ, LeCluyse EL, Kim RB, Meier PJ, and Brouwer KL (2004)

P-glycoprotein expression, localization, and function in sandwich-cultured primary rat

and human hepatocytes: relevance to the hepatobiliary disposition of a model opioid

peptide. *Pharm Res* **21**:1294–1302.

Ito K, Iwatsubo T, Kanamitsu S, Nakajima Y, and Sugiyama Y (1998) Quantitative prediction of in vivo drug clearance and drug interactions from in vitro data on metabolism, together with binding and transport. *Annu Rev Pharmacol Toxicol* **38**:461–499.

Iwatsubo T, Hirota N, Ooie T, Suzuki H, Shimada N, Chiba K, Ishizaki T, Green CE, Tyson CA, and Sugiyama Y (1997) Prediction of in vivo drug metabolism in the human liver from in vitro metabolism data. *Pharmacol Ther* **73**:147–171.

Kato Y, Suzuki H, and Sugiyama Y (2002) Toxicological implications of hepatobiliary transporters. *Toxicology* **27**:287–290.

Kato Y, Takahara S, Kato S, Kubo Y, Sai Y, Tamai I, Yabuuchi H, Tsuji A (2008) Involvement of multidrug resistance-associated protein 2 (Abcc2) in molecular weight-dependent biliary excretion of beta-lactam antibiotics. *Drug Metab Dispos* **36**: 1088-1096.

Kitamura S, Maeda K, Wang Y, and Sugiyama Y (2008) Involvement of multiple transporters in the hepatobiliary transport of rosuvastatin. *Drug Metab Dispos* **36**:2014–2023.

LeCluyse EL, Audus KL, and Hochman JH (1994) Formation of extensive canalicular networks by rat hepatocytes cultured in collagen-sandwich configuration. *Am J Physiol* **266**:C1764–1774.

Levine WG (1978) Biliary excretion of drugs and other xenobiotics. *Annu Rev Pharmacol Toxicol* **18**:81–96.

Li N, Singh P, Mandrell KM, and Lai Y (2010) Improved extrapolation of hepatobiliary clearance from in vitro sandwich cultured rat hepatocytes through absolute quantification of hepatobiliary transporters. *Mol Pharm* **7**:630–641.

Liu X, Chism JP, LeCluyse EL, Brouwer KR, and Brouwer KL (1999a) Correlation of biliary excretion in sandwich-cultured rat hepatocytes and in vivo in rats. *Drug Metab Dispos* **27**:637–644.

Liu X, LeCluyse EL, Brouwer KR, Gan LS, Lemasters JJ, Stieger B, Meier PJ, and Brouwer KL (1999b) Biliary excretion in primary rat hepatocytes cultured in a collagen-sandwich configuration. *Am J Physiol* **277**:G12–21.

Muraoka I, Hasegawa T, Nadai M, Wang L, Haghgoo S, Tagaya O, and Nabeshima T (1995) Biliary and renal excretions of cefpiramide in Eisai hyperbilirubinemic rats. *Antimicrob Agents Chemother* **39**: 70-74.

Nakakariya M, Shimada T, Irokawa M, Koibuchi H, Iwanaga T, Yabuuchi H, Maeda T, and Tamai I (2008) Predominant contribution of rat organic anion transporting

polypeptide-2 (Oatp2) to hepatic uptake of beta-lactam antibiotics. *Pharm Res* **25**:578–585.

Nakagomi-Hagihara R, Nakai D, Kawai K, Yoshigae Y, Tokui T, Abe T, and Ikeda T (2006) OATP1B1, OATP1B3, and mrp2 are involved in hepatobiliary transport of olmesartan, a novel angiotensin II blocker. *Drug Metab Dispos* **34**:862–869.

Olsavsky KM, Page JL, Johnson MC, Zarbl H, Strom SC, and Omiecinski CJ (2007) Gene expression profiling and differentiation assessment in primary human hepatocyte cultures, established hepatoma cell lines, and human liver tissues. *Toxicol Appl Pharmacol* **222**:42–56.

Rollins DE and Klaassen CD (1979) Biliary excretion of drugs in man. *Clin Pharmacokinet* **4**:368–379.

Sasaki M, Suzuki H, Aoki J, Ito K, Meier PJ, Sugiyama Y (2004) Prediction of in vivo biliary clearance from the in vitro transcellular transport of organic anions across a double-transfected Madin-Darby canine kidney II monolayer expressing both rat organic anion transporting polypeptide 4 and multidrug resistance associated protein 2. *Mol Pharmacol* **66**: 450-459.

Seglen PO (1976) Preparation of isolated rat liver cells. *Methods Cell Biol* **13**:29–83.

Takayanagi M, Sano N, Takikawa H (2005) Biliary excretion of olmesartan, an anigotensin II

receptor antagonist, in the rat. *J Gastroenterol Hepatol* **20**: 784-788.

Talamini MA, Kappus B, and Hubbard A (1997) Repolarization of hepatocytes in culture.

Hepatology **25**:167–172.

Watanabe T, Maeda K, Kondo T, Nakayama H, Horita S, Kusuhara H, and Sugiyama Y

(2009) Prediction of the hepatic and renal clearance of transporter substrates in

rats using in vitro uptake experiments. *Drug Metab Dispos* **37**:1471–1479.

Watanabe T, Kusuhara H, Maeda K, Kanamaru H, Saito Y, Hu Z, and Sugiyama Y (2010a)

Investigation of the rate-determining process in the hepatic elimination of

HMG-CoA reductase inhibitors in rats and humans. *Drug Metab Dispos* **38**:215–222.

Watanabe T, Kusuhara H, and Sugiyama Y (2010b) Application of physiologically based

pharmacokinetic modeling and clearance concept to drugs showing

transporter-mediated distribution and clearance in humans. *J Pharmacokinet

Pharmacodyn* **37**:575–590.

Yamano K, Yamamoto K, Kotaki H, Takedomi S, Matsuo H, Sawada Y, and Iga T (1999)

Correlation between in vivo and in vitro hepatic uptake of metabolic inhibitors of cytochrome P-450 in rats. *Drug Metab Dispos* **27**:1225–1231.

Yamashiro W, Maeda K, Hirouchi M, Adachi Y, Hu Z, and Sugiyama Y (2006) Involvement of transporters in the hepatic uptake and biliary excretion of valsartan, a selective antagonist of the angiotensin II AT1-receptor, in humans. *Drug Metab Dispos* **34**:1247–1254.

Zhang P, Tian X, Chandra P, and Brouwer KL (2005) Role of glycosylation in trafficking of Mrp2 in sandwich-cultured rat hepatocytes. *Mol Pharmacol* **67**:1334–1341.

Footnotes

This research was supported in part by the grant "Research on Publicly Essential Drugs and

Medical devices" from the Japan Health Sciences Foundation.

Legend for Figures and Tables

Fig. 1   Phase contrast and fluorescent images after incubation with CDF diacetate in sandwich-cultured rat hepatocytes (SCRH).   SCRH were incubated with CDF diacetate (1 μmol/L) in standard buffer (B) and (–) HBSS (C) for 20 min.   A: phase contrast image of SCRH after culture for 4 days.   Canalicular lumen is indicated by arrows.

Fig. 2   Accumulation of rosuvastatin (0.5 μmol/L) (A), pravastatin (0.5 μmol/L) (B), valsartan (1 μmol/L) (C), olmesartan (1 μmol/L) (D), cefmetazole (25 μmol/L) (E), cefoperazone (20 μmol/L) (F), cefpiramide (10 μmol/L) (G), and topotecan (5 μmol/L) (H) in SCRH.   Each substrate was preincubated in standard buffer (solid bars) and (–) HBSS (white bars).   Data represent the mean + S.D. (n = 3).

Fig. 3   Relationship between *in vitro* $CL_{bile,app}$ predicted from SCRH and *in vivo* $CL_{bile,app}$ with rosuvastatin (●), pravastatin (□), valsartan (○), olmesartan (◊), cefmetazole (■), cefoperazone (▲), cefpiramide (▼) and topotecan (▲).   Predicted $CL_{bile,app}$ was calculated based on plasma total (A) or unbound concentrations (B).   Data represent the mean (n = 3).

Fig. 4 Plasma concentration- (A) and bile amount- (B) time profile of rosuvastatin (●),

pravastatin (□), valsartan (○), olmesartan (◊), cefmetazole (■), cefoperazone (▲), cefpiramide

(▼) and topotecan (▲) during continuous intravenous infusion to rats. Data represent the

mean ± S.D. (n = 5).

Fig. 5 Relationship between *in vitro* $CL_{bile,int}$ and *in vivo* $CL_{bile,int}$ with rosuvastatin (●),

pravastatin (□), valsartan (○), olmesartan (◊), cefmetazole (■), cefoperazone (▲), cefpiramide

(▼), and topotecan (▲). *In vivo* and *in vitro* $CL_{bile,int}$ were calculated using eq. 7 and 8,

respectively. Data represent the mean ± S.D. (n = 3 and 5 for *in vitro* and *in vivo* experiments,

respectively).

Fig. 6 Accumulation profiles of rosuvastatin (A) and pravastatin (B). Each substrate (4

μmol/L) was preincubated in standard buffer (●) and (-) HBSS (○). Data represent the mean ±

S.D. (n = 3).

Table 1   Kinetic parameters of biliary excretion for compounds in SCRH

Compound	BEI (%)			$CL_{bile,app}$ (mL/h/kg)			Predicted $CL_{bile,app}$ (mL/h/kg)					
							From eq. 4			From eq. 5		
Rosuvastatin	40.0	±	3.5	2794.9	±	419.2	1252.0	±	353.8	93.8	±	14.6
Pravastatin	38.8	±	3.6	387.3	±	57.0	330.8	±	55.6	243.7	±	39.5
Valsartan	13.6	±	3.6	471.6	±	145.8	390.4	±	137.0	1.4	±	0.4
Olmesartan	6.6	±	2.4	314.0	±	120.2	275.8	±	114.2	3.1	±	1.2
Cefmetazole	N.A.			N.A			N.A.			N.A.		
Cefoperazone	29.9	±	5.7	8.8	±	2.4	8.7	±	2.4	3.8	±	1.0
Cefpiramide	25.4	±	5.8	5.9	±	1.8	5.9	±	1.8	0.9	±	0.3
Topotecan	18.2	±	4.3	29.2	±	8.2	28.8	±	8.2	21.6	±	6.1

BEI and $CL_{bile,app}$ values were calculated according to eq. 2 and 3 based on the accumulation for 15 min incubation, respectively

Each value represents the mean ± S.D. (n = 3).

N.A.: not available

Table 2   Pharmacokinetic and biliary excretion parameters

Compound	CL_{total} (mL/h/kg)	$CL_{bile,app}$ (mL/h/kg)	Biliary excretion (% of dose)	$f_{u,p}$
Rosuvastatin	1680[a]	1450	86.3[a]	0.035
Pravastatin	2622[a]	1644	62.7[a]	0.705
Valsartan	252[a]	210	83.2[a]	0.003
Olmesartan	194[b]	168	86.8[b]	0.010
Cefmetazole	576[a]	373	64.7[a]	0.738
Cefoperazone	804[a]	603	75.0[a]	0.429
Cefpiramide	489[c]	283	57.8[c]	0.158
Topotecan	2409[d]	318	13.2[d]	0.747

$CL_{bile,app}$ values were calculated according to eq. 6.

Each value represents the mean (n = 3 or 4).

[a] Fukuda et al. (2008)

[b] Watanabe et al. (2009)

[c] Muraoka et al. (1995)

[d] Li et al. (2010)

Table 3 *In vivo* **CL$_{bile,int}$ of drugs in rats**

Compound	CL$_{bile,int}$ (mL/h/kg)		
Rosuvastatin	150.3	±	30.2
Pravastatin	403.4	±	94.3
Valsartan	71.1	±	15.6
Olmesartan	66.8	±	6.0
Cefmetazole	214.0	±	58.2
Cefoperazone	323.1	±	58.5
Cefpiramide	201.4	±	15.9
Topotecan	27.5	±	2.5

CL$_{bile,int}$ values were calculated according to eq. 7.

Each value represents the mean ± S.D. (n = 5).

43

Table 4   Kinetic parameters of drugs in SCRH and rat liver

Compound	In SCRH			In vivo	
	Concentration in medium (μmol/L)	Concentration in hepatocytes[a] (μmol/L)	$CL_{bile,int}$ (mL/h/kg)	Concentration in liver (μmol/L)	$CL_{bile,int}$ (mL/h/kg)
Rosuvastatin	0.5	11.8	111.6	7.1	150.3
Pravastatin	0.5	1.9	106.2	1.9	403.4
Valsartan	1	17.5	26.5	17.4	71.1
Olmesartan	1	26.0	11.9	19.1	66.8
Cefmetazole	25	11.4	N.A.	5.1	214.0
Cefoperazone	20	2.6	72.1	2.5	323.1
Cefpiramide	10	1.0	57.7	2.6	201.4
Topotecan	5	3.3	37.5	6.9	27.5

In vivo and *in vitro* $CL_{bile,int}$ values were calculated according to eq. 7 and 8, respectively.

[a] Compound concentration in hepatocytes were calculated according to eq. 9.

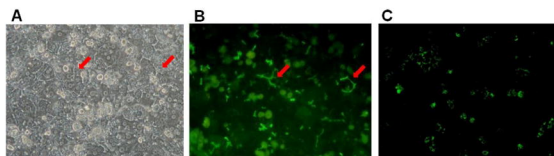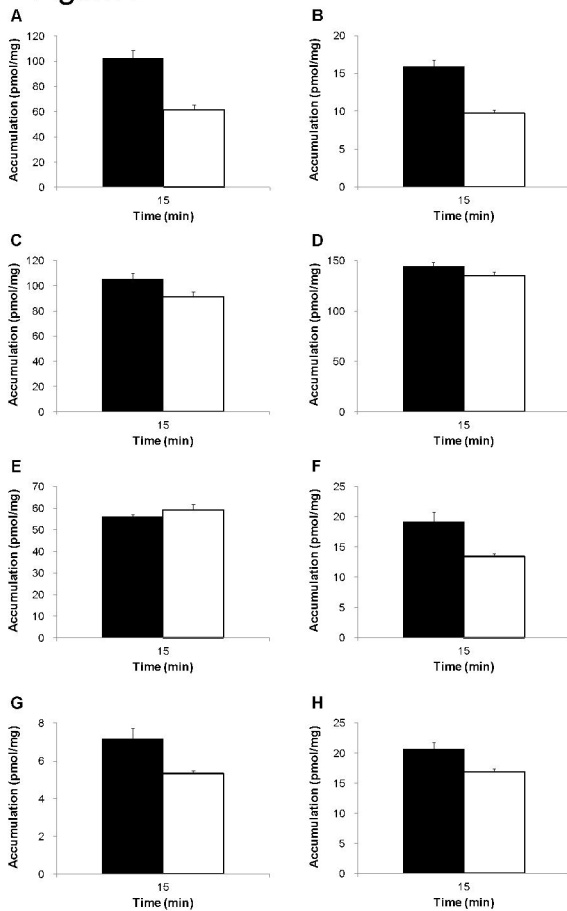Each value represents the mean (n = 3 and 5 for *in vitro* and *in vivo* experiments, respectively).
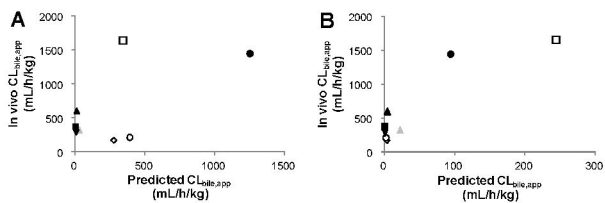
N.A.: not available

44

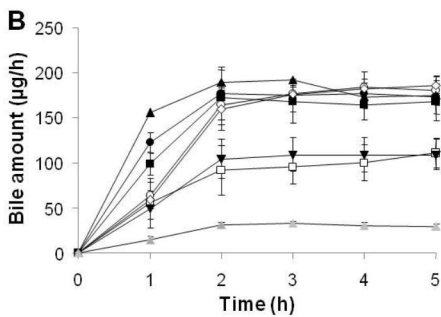Figure 1

Figure 2

Figure 3

Figure 4

Figure 5

Figure 6